

# Improvement of heavy-heavy current for calculation of $\bar{B} \rightarrow D^{(*)} \ell \bar{\nu}$ form factors using Oktay-Kronfeld heavy quarks

Jon A. Bailey<sup>1</sup>, Yong-Chull Jang<sup>2,3</sup>, Weonjong Lee<sup>1,\*</sup>, Jaehoon Leem<sup>1,\*\*</sup>, and (LANL-SWME Collaboration)

<sup>1</sup>Lattice Gauge Theory Research Center, CTP, Department of Physics and Astronomy, Seoul National University, Seoul 08826, South Korea

<sup>2</sup>Los Alamos National Laboratory, Theoretical Division T-2, Los Alamos, New Mexico 87545, USA

<sup>3</sup>Brookhaven National Laboratory, Department of Physics, Upton, New York 11973, USA

**Abstract.** The CKM matrix element  $|V_{cb}|$  can be extracted by combining data from experiments with lattice QCD results for the semileptonic form factors for the  $\bar{B} \rightarrow D^{(*)} \ell \bar{\nu}$  decays. The Oktay-Kronfeld (OK) action was designed to reduce heavy-quark discretization errors to below 1%, or through  $\mathcal{O}(\lambda^3)$  in HQET power counting. Here we describe recent progress on bottom-to-charm currents improved to the same order in HQET as the OK action, and correct formerly reported results of our matching calculations, in which the operator basis was incomplete.

## 1 Introduction

The Cabibbo-Kobayashi-Maskawa (CKM) matrix element  $|V_{cb}|$  normalizes the unitarity triangle, and the uncertainty in  $|V_{cb}|$  propagates to many quark-flavor observables such as  $\varepsilon_K$  [1], limiting the precision of constraints on the CKM matrix. Accordingly, determinations of  $|V_{cb}|$  with greater precision are essential to improve these constraints and understand the mechanism underlying the dynamics and CP violation of the quark-flavor sector.

$|V_{cb}|$  can be extracted from the exclusive semileptonic decays  $\bar{B} \rightarrow D \ell \bar{\nu}$  and  $\bar{B} \rightarrow D^* \ell \bar{\nu}$ . The approach involves combining the branching fractions from experiments with the form factors calculated on the lattice [2–4]. The calculations of the form factors by the authors of Refs. [2, 3] have so far relied on the Wilson clover action [5] interpreted nonrelativistically *via* HQET [6, 7] to control the discretization errors of the charm and bottom quarks, with final errors of 2 – 5% [2, 3]. Given precise lattice inputs for the form factors, the data from BELLE2 at KEK will allow extractions of  $|V_{cb}|$  at the subpercent level.

The Oktay-Kronfeld (OK) action is an improved Wilson action developed to reduce the discretization errors of heavy quarks to below 1% even on lattices with spacings as large as  $a \approx 0.12$  fm [8]. For quark masses large compared with the lattice cutoff, the OK action possesses heavy-quark symmetry. To design the OK action, it is convenient to use tools of HQET [9] and NRQCD [10] to quantify the heavy-quark discretization errors and to tune the action to the continuum limit [7, 8]. For

---

\*e-mail: wlee@snu.ac.kr

\*\*Speaker

heavy-light systems, HQET power counting is appropriate, while for quarkonia, NRQCD provides the appropriate power counting [8]. The OK action includes all dimension-five, all dimension-six, and some dimension-seven bilinears through  $\mathcal{O}(\lambda^3)$  in HQET. Estimates of truncation errors indicate that one-loop matching of dimension-five bilinears and tree-level matching of the dimension-six and -seven operators should suffice for the target precision [8]. Numerical tests of the tree-level matched, tadpole-improved OK action indicate significant improvement even without one-loop matching of the dimension-five bilinears [11].

To reduce systematically heavy-quark discretization errors in calculations of the  $\bar{B} \rightarrow D^{(*)} \ell \bar{\nu}$  form factors, the flavor-changing ( $b \rightarrow c$ ) currents must also be improved through  $\mathcal{O}(\lambda^3)$  in HQET. In addition to the dimension-four improvement term introduced in Ref. [6], the improved current must include dimension-five and -six operators. In Sec. 2, we introduce an improved current in terms of an improved quark field. In Sec. 3, we write down matching conditions and describe a tree-level matching calculation *via* HQET. In Sec. 4, we discuss the results. We add two appendices to describe some technical details.

## 2 $\mathcal{O}(\lambda^3)$ -improved quark field

To take advantage of using the OK action in calculating form factors of  $\bar{B} \rightarrow D^{(*)} \ell \bar{\nu}$  semileptonic decays, the improvement of flavor-changing currents should be performed to the same level, *i.e.*, through  $\mathcal{O}(\lambda^3)$  in HQET power counting. In case of improvement through  $\mathcal{O}(\lambda)$ , the current improvement was performed by introducing an improved quark field [6],

$$J_\Gamma^{\text{lat}} \equiv \bar{\Psi}_{Ic} \Gamma \Psi_{Ib}, \quad (1)$$

where  $\Psi_{If}$  is the improved quark field and  $\Gamma$  represents the Dirac spin structure.

Our basic assumption is that improving quark fields is sufficient for the improvement of currents at the tree level [6]. To improve the current up to  $\mathcal{O}(\lambda^3)$ , we extend the construction of the improved quark fields to higher dimension. To obtain the results of Ref. [12], we assumed an ansatz for the improved quark field motivated by the symmetries of the theory and the operators appearing in the OK action, which turns out to be insufficient because two operators were missing from the operator basis. These two additional operators are essential to match four quark matrix elements at  $\mathcal{O}(\mathbf{p})$  in the external heavy-quark momentum and at  $\mathcal{O}(\lambda^3)$  in HQET.

Considering the Foldy-Wouthuysen-Tani (FWT) transformation on the continuum quark action, we are led to include two new operators in the ansatz. To  $\mathcal{O}(1/m^3)$ , the FWT transformation [13] used to obtain the  $\mathcal{O}(1/m^3)$  HQET Lagrangian [14] from the Dirac action is

$$Q = \left[ 1 - \frac{1}{2m} \boldsymbol{\gamma} \cdot \mathbf{D} + \frac{1}{8m^2} \mathbf{D}^2 + \frac{i}{8m^2} \boldsymbol{\Sigma} \cdot \mathbf{B} + \frac{1}{4m^2} \boldsymbol{\alpha} \cdot \mathbf{E} - \frac{\{\gamma_4 D_4, \boldsymbol{\alpha} \cdot \mathbf{E}\}}{8m^3} - \frac{3\{\boldsymbol{\gamma} \cdot \mathbf{D}, \mathbf{D}^2\}}{32m^3} \right. \\ \left. - \frac{3\{\boldsymbol{\gamma} \cdot \mathbf{D}, i\boldsymbol{\Sigma} \cdot \mathbf{B}\}}{32m^3} - \frac{\{\boldsymbol{\gamma} \cdot \mathbf{D}, \boldsymbol{\alpha} \cdot \mathbf{E}\}}{16m^3} + \frac{[\gamma_4 D_4, \mathbf{D}^2]}{16m^3} + \frac{[\gamma_4 D_4, i\boldsymbol{\Sigma} \cdot \mathbf{B}]}{16m^3} \right] h + \mathcal{O}(1/m^4), \quad (2)$$

where  $Q$  is the Dirac field, and  $h$  is the heavy quark field in HQET. Accordingly, we consider an ansatz for the improved field that includes all operators analogous to those in the continuum FWT transformation of Eq. (2) as well as those corresponding to lattice artifacts,

$$\Psi_I(x) = e^{m_1/2} \left[ 1 + d_1 \boldsymbol{\gamma} \cdot \mathbf{D}_{\text{lat}} + \frac{1}{2} d_2 \Delta^{(3)} + \frac{1}{2} i d_B \boldsymbol{\Sigma} \cdot \mathbf{B}_{\text{lat}} + \frac{1}{2} d_E \boldsymbol{\alpha} \cdot \mathbf{E}_{\text{lat}} + \frac{1}{6} d_3 \gamma_i D_{\text{lat},i} \Delta_i + d_{EE} \{\gamma_4 D_{\text{lat},4}, \boldsymbol{\alpha} \cdot \mathbf{E}_{\text{lat}}\} \right. \\ \left. + \frac{1}{2} d_4 \{\boldsymbol{\gamma} \cdot \mathbf{D}_{\text{lat}}, \Delta^{(3)}\} + d_5 \{\boldsymbol{\gamma} \cdot \mathbf{D}_{\text{lat}}, i\boldsymbol{\Sigma} \cdot \mathbf{B}_{\text{lat}}\} + d_{rE} \{\boldsymbol{\gamma} \cdot \mathbf{D}_{\text{lat}}, \boldsymbol{\alpha} \cdot \mathbf{E}_{\text{lat}}\} + d_6 [\gamma_4 D_{\text{lat},4}, \Delta^{(3)}] \right]$$

$$+ d_7[\gamma_4 D_{\text{lat},4}, i\mathbf{\Sigma} \cdot \mathbf{B}_{\text{lat}}] + d_{z_3}\gamma \cdot (\mathbf{D}_{\text{lat}} \times \mathbf{B}_{\text{lat}} + \mathbf{B}_{\text{lat}} \times \mathbf{D}_{\text{lat}}) + d_{z_E}\gamma_4(\mathbf{D}_{\text{lat}} \cdot \mathbf{E}_{\text{lat}} - \mathbf{E}_{\text{lat}} \cdot \mathbf{D}_{\text{lat}})\Big]\psi(x), \quad (3)$$

where we set  $a = 1$  for convenience.

The terms in Eq. (3) with coefficients  $d_3$ ,  $d_{z_3}$ , and  $d_{z_E}$  have no analogues in Eq. (2). The  $d_3$  term breaks rotational symmetry and is necessary to remedy symmetry breaking. In Eq. (2), the  $d_{z_3}$  and  $d_{z_E}$  terms are absent, which reflects the fact that they vanish at tree level, as reported in Ref. [12]. Comparing Eq. (3) with the ansatz of Ref. [12], we observe that the terms for  $d_6$  and  $d_7$  are new. These correspond to the last two terms in the FWT transformation of Eq. (2). In our previous paper [12], our calculation at  $\mathcal{O}(\mathbf{p})$  was incomplete, so that we missed the  $d_6$  and  $d_7$  terms. An explicit matching calculation of the lattice and continuum four-quark matrix elements *via* HQET indicates that the ansatz with the  $d_6$  and  $d_7$  terms suffices to match these matrix elements at tree level through  $\mathcal{O}(\lambda^3)$ .

### 3 Matching calculation

In this section we describe how to determine the coefficients  $d_i$  in the improved quark field. We match the following four-quark matrix elements at tree level between the lattice theory and continuum QCD,

$$\langle \ell(\eta_2, p_2)c(\eta', p') | \bar{\Psi}_{lc}\Gamma\Psi_{lb} | b(\eta, p)\ell(\eta_1, p_1) \rangle_{\text{Lat}} \leftrightarrow \langle \ell(\eta_2, p_2)c(\eta', p') | \bar{c}\Gamma b | b(\eta, p)\ell(\eta_1, p_1) \rangle_{\text{Con}}, \quad (4)$$

where  $\ell$  represents a light spectator quark, and  $c$  and  $b$  indicate a charm quark and bottom quark, respectively. At tree level gluon exchange may occur at either the  $b$ -quark line or the  $c$ -quark line. The matching conditions for the coefficients in the improved  $b$ - and  $c$ -quark fields factorize at the tree level, and the coefficients in each field are determined separately. Hence, we consider only gluon exchange at the  $b$ -quark line, because the results for the  $c$ -quark field are formally identical.

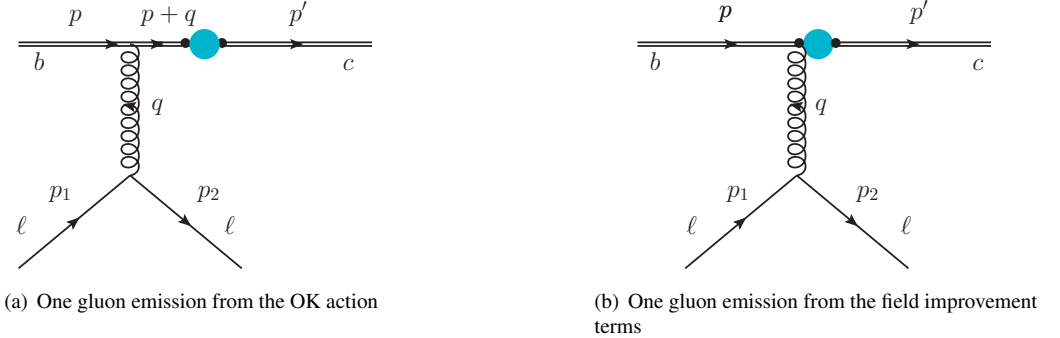


**Figure 1.** The tree level, lattice diagrams with gluon exchange at the external  $b$ -quark line. The dot without a gluon line in (a) diagram represents the zero-gluon vertex, and the dot with a gluon line in (b) diagram represents the one-gluon vertex from the improved quark field.

The corresponding lattice Feynman diagrams are given in Figure 1. One gluon exchange diagrams show up in two different ways: The one-gluon vertex of the action in Fig. 1 (a) can emit a gluon, and the improvement vertex of the  $b$  quark in Fig. 1 (b) can do it, too. Comparing these lattice diagrams with the continuum diagrams provides the following matching conditions for the improved  $b$ -quark field,

$$n_\mu(q)\left[R_b^{(0)}(p+q)S^{\text{lat}}(p+q)(-gt^a)\Lambda_\mu(p+q, p) + (-gt^a)R_{b\mu}^{(1)}(p+q, p)\right]\mathcal{N}_b(\mathbf{p})u_b^{\text{lat}}(\eta, \mathbf{p})$$

$$= S(p+q)(-gt^a)\gamma_\mu \sqrt{\frac{m_b}{E_b}} u_b(\eta, \mathbf{p}), \quad (5)$$

where the LHS (RHS) represents the lattice (continuum) part. Here,  $q$  is the four-momentum of the gluon, and  $\mu$  and  $a$  are the Lorentz and color indices, respectively.  $n_\mu(q) = 2 \sin(\frac{1}{2}q_\mu)/q_\mu$  is the wave function factor for the lattice gluon.  $\mathcal{N}_b(p)$  is the lattice spinor normalization factor for the  $b$  quark, which corresponds to  $\sqrt{m_b/E_b}$  in the continuum.  $S_b$  and  $S_b^{\text{lat}}$  are the  $b$ -quark propagator in the continuum and on the lattice, respectively.  $\Lambda_\mu$  is the one-gluon vertex of the OK action [8].

The contributions of the improvement parameters  $d_i$  enter through the zero-gluon vertex  $R_b^{(0)}$  and the one-gluon vertex  $R_{b\mu}^{(1)}$  from the improved quark field. The explicit formulas were given in Ref. [12]. The results for  $R_{b\mu}^{(1)}$  must be corrected for the addition of the  $d_6$  and  $d_7$  terms; the results for  $R_b^{(0)}$  are unchanged. Then we have

$$R_{bi}^{(1)} = R_{bi}^{(1)\text{Ref. [12]}} + e^{m_{1,b}} [\sin(p_4 + q_4) - \sin p_4] \left[ 2d_6\gamma_4 \sin(p_i + \frac{1}{2}q_i) - i\epsilon_{ijk}d_7 \cos \frac{1}{2}q_i \sin q_j \Sigma_k \gamma_4 \right], \quad (6)$$

$$R_{b4}^{(1)} = R_{b4}^{(1)\text{Ref. [12]}} + 4e^{m_{1,b}} d_6 \cos(p_4 + \frac{1}{2}q_4) \sum_{j=1}^3 \left[ \sin^2 \frac{1}{2}(p_j + q_j) - \sin^2 \frac{1}{2}p_j \right]. \quad (7)$$

The spatial momentum of the  $b$  quark  $\mathbf{p}$  and the four-momentum of the gluon  $q$  are of order  $\Lambda_{\text{QCD}}$ , small compared to  $m_b$  and the lattice cut-off scale  $1/a$ . Expanding both sides of Eq. (5) in powers of  $\mathbf{p}/m_b$ ,  $q/m_b$ ,  $\mathbf{p}a$ , and  $qa$ , all the terms are organized by powers of  $\lambda \sim a\Lambda_{\text{QCD}} \sim \Lambda_{\text{QCD}}/2m_b$ . Expanding through  $\mathcal{O}(\lambda^3)$ , both sides of Eq. (5) can be sorted into terms of the zero- and one-gluon vertices of the lattice and continuum HQET Lagrangians and flavor-changing currents [7]. Explicitly, the LHS of Eq. (5) can be rewritten as follows,

$$\left[ R_{\text{HQ},\mu}^{\text{lat,(1)}}(p+q, p) + \sum_n R_{\text{HQ}}^{\text{lat,(0)}}(p+q) \left( \frac{1}{iP_4^{\text{lat}}} \Lambda_{\text{HQ}}^{\text{lat,(0)}}(p+q) \right)^n \frac{1}{iP_4^{\text{lat}}} \Lambda_{\text{HQ},\mu}^{\text{lat,(1)}}(p+q, p) \right] (-gt^a) u(\eta, 0), \quad (8)$$

where  $P_4^{\text{lat}} \equiv p_4^{\text{lat}} - im_{1,b} + q_4$  is the time component of the residual momentum of the internal  $b$  quark.  $\Lambda_{\text{HQ}}^{\text{lat,(0)}}$  and  $\Lambda_{\mu,\text{HQ}}^{\text{lat,(1)}}$  are the zero- and one-gluon vertices of the lattice HQET Lagrangian, respectively.  $R_{\text{HQ}}^{\text{lat,(0)}}$  and  $R_{\text{HQ},\mu}^{\text{lat,(1)}}$  are the zero- and one-gluon vertices from the lattice HQET current, including the correction terms analogous to those in the FWT transformation of Eq. (2). Expressions for the vertices are given in Appendix A. The external  $b$  quark is on shell,

$$p_4^{\text{lat}} - im_{1,b} = i \left[ \frac{1}{2m_{2,b}} \mathbf{p}^2 - \frac{1}{6} w_{4,b} \sum_i p_i^4 - \frac{1}{8m_{4,b}^2} \mathbf{p}^4 + \dots \right], \quad (9)$$

where matching the dispersion relation requires  $m_{2,b} = m_{4,b} = m_b$  and  $w_{4,b} = 0$  [6]. In terms of the continuum HQET vertices, the form of the RHS of Eq. (5) is the same as Eq. (8), with all superscripts “lat” dropped.

The matching condition Eq. (5) is that the lattice HQET vertices are equal to those in the continuum as follows,

$$\Lambda_{\text{HQ}}^{\text{lat,(0)}}(p+q, p) = \Lambda_{\text{HQ}}^{(0)}(p+q, p), \quad \Lambda_{\text{HQ},\mu}^{\text{lat,(1)}}(p+q, p) = \Lambda_{\text{HQ},\mu}^{(1)}(p+q, p), \quad (10)$$

$$R_{\text{HQ}}^{\text{lat,(0)}}(p+q, p) = R_{\text{HQ}}^{(0)}(p+q, p), \quad R_{\text{HQ},\mu}^{\text{lat,(1)}}(p+q, p) = R_{\text{HQ},\mu}^{(1)}(p+q, p). \quad (11)$$

From the explicit expressions for  $\Lambda_{\text{HQ}}^{(\text{lat}), (0)}$  and  $\Lambda_{\text{HQ},\mu}^{(\text{lat}), (1)}$ , one can show that Eqs. (10) are satisfied automatically from matching the OK action [8]. This consistency is highly non-trivial. The OK action

given in Ref. [8] passes multiple consistency tests up to  $\mathcal{O}(\lambda^3)$ . By imposing Eqs. (11) at each order through  $\mathcal{O}(\lambda^3)$ , we obtain a complete set of constraints to determine all the improvement parameters  $d_i$  in Eq. (3).

## 4 Results

In summary, by matching the four-quark matrix elements of Eq. (4), the current operator defined by the improved quark field of Eq. (3) is matched to the lattice HQET current:

$$\bar{\Psi}_{Ic}\Gamma\Psi(x)_{Ib} \doteq \bar{h}_c\mathcal{U}_{\text{lat}}^c\Gamma\mathcal{W}_{\text{lat}}^bh_b, \quad (12)$$

where

$$\begin{aligned} \mathcal{W}_{\text{lat}}^b = & \left[ 1 - \frac{1}{2m_{3,b}}\boldsymbol{\gamma} \cdot \mathbf{D} + \frac{1}{8m_{D_{\perp}^2,b}}\mathbf{D}^2 + \frac{i}{8m_{sB,b}}\boldsymbol{\Sigma} \cdot \mathbf{B} + \frac{1}{4m_{\alpha E,b}}\boldsymbol{\alpha} \cdot \mathbf{E} - \frac{\{\gamma_4 D_4, \boldsymbol{\alpha} \cdot \mathbf{E}\}}{8m_{\alpha EE,b}^3} - \frac{3\{\boldsymbol{\gamma} \cdot \mathbf{D}, \mathbf{D}^2\}}{32m_{\gamma DD_{\perp}^2,b}^3} \right. \\ & \left. - \frac{3\{\boldsymbol{\gamma} \cdot \mathbf{D}, i\boldsymbol{\Sigma} \cdot \mathbf{B}\}}{32m_{sB,b}^3} - \frac{\{\boldsymbol{\gamma} \cdot \mathbf{D}, \boldsymbol{\alpha} \cdot \mathbf{E}\}}{16m_{\alpha EE,b}^3} + \frac{[\gamma_4 D_4, \mathbf{D}^2]}{16m_{6,b}^3} + \frac{[\gamma_4 D_4, i\boldsymbol{\Sigma} \cdot \mathbf{B}]}{16m_{7,b}^3} + dw_{1,b} \sum_i \gamma_i D_i^3 + \frac{dw_{2,b}}{8}[\boldsymbol{\gamma} \cdot \mathbf{D}, \mathbf{D}^2] \right], \end{aligned} \quad (13)$$

and  $dw_{i,b} = 0$  and  $m_{i,b} = m_b$  are required for matching. Explicit expressions for  $dw_{i,b}$  and  $m_{i,b}$  are given in Appendix B. The operators in Eq. (13) are the continuum operators of the HQET description of lattice QCD, and the coefficients contain the lattice artifacts of the heavy quark. Although the matching calculation *via* HQET is distinct from our previous calculations [12], the results for all improvement parameters except  $d_{r_E}$  (and the new coefficients  $d_6$  and  $d_7$ ) are the same.

The results for the improvement parameters are as follows. Two of the improvement parameters are zero:  $d_{z_3} = d_{z_E} = 0$ . We omit the flavor index ( $b$  or  $c$ ) for notational convenience. The remaining results are

$$d_1 = \frac{\zeta(1+m_0)}{m_0(2+m_0)} - \frac{1}{2m}, \quad d_2 = \frac{2\zeta(1+m_0)}{m_0(2+m_0)}d_1 - \frac{r_s\zeta}{2(1+m_0)} - \frac{\zeta^2(1+m_0)^2}{m_0^2(2+m_0)^2} + \frac{1}{4m^2}, \quad (14)$$

$$d_3 = w_3 - d_1, \quad d_B = \frac{2\zeta(1+m_0)}{m_0(2+m_0)}d_1 - \frac{c_B\zeta}{2(1+m_0)} - \frac{\zeta^2(1+m_0)^2}{m_0^2(2+m_0)^2} + \frac{1}{4m^2}, \quad (15)$$

$$d_E = -\frac{2(1+m_0)\zeta}{m_0^2(2+m_0)^2} - \frac{(m_0+1)\zeta c_E}{m_0(2+m_0)} + \frac{1}{2m^2}, \quad d_{r_E} = \frac{1}{16m_3m_{\alpha E}^2} + \frac{d_1 d_E}{4} - \frac{1}{16m^3}, \quad (16)$$

$$d_{EE} = \frac{1+m_0}{(m_0^2+2m_0+2)} \left[ -\frac{1}{4m^3} + \frac{\zeta(1+m_0)(m_0^2+2m_0+2)}{[m_0(2+m_0)]^3} + \frac{\zeta c_E(1+m_0)}{[m_0(2+m_0)]^2} + \frac{(2+2m_0+m_0^2)c_{EE}}{m_0(2+m_0)} \right], \quad (17)$$

$$\begin{aligned} d_4 = & \frac{\zeta^3(m_0^3+3m_0^2+5m_0+3)}{2m_0^3(2+m_0)^3} + \frac{r_s\zeta^2(3m_0^2+6m_0+4)}{4m_0^2(2+m_0)^2} + \frac{2(1+m_0)c_2}{m_0(2+m_0)} - \frac{(1+m_0)^2\zeta^2}{2m_0^2(2+m_0)^2}d_1 \\ & - \frac{r_s\zeta}{4(1+m_0)}d_1 + \frac{(1+m_0)\zeta d_2}{2m_0(2+m_0)} - \frac{3}{16m^3}, \end{aligned} \quad (18)$$

$$\begin{aligned} d_5 = & \frac{1}{2} \left[ \frac{\zeta^3(m_0^3+3m_0^2+5m_0+3)}{2m_0^3(2+m_0)^3} + \frac{c_B\zeta^2(3m_0^2+6m_0+4)}{4m_0^2(2+m_0)^2} + \frac{2(1+m_0)c_3}{m_0(2+m_0)} - \frac{(1+m_0)^2\zeta^2}{2m_0^2(2+m_0)^2}d_1 \right. \\ & \left. - \frac{c_B\zeta}{4(1+m_0)}d_1 + \frac{(1+m_0)\zeta d_B}{2m_0(2+m_0)} - \frac{3}{16m^3} \right], \end{aligned} \quad (19)$$

$$d_6 = \frac{2(1+m_0)}{(m_0^2+2m_0+2)} \left[ -\frac{1}{16m_3m_{\alpha E}^2} + \frac{\zeta^2 c_E}{4m_0(2+m_0)} - \frac{\zeta c_{EE}(m_0^2+2m_0+2)}{2m_0(1+m_0)(2+m_0)} - \frac{d_E}{4} \left( d_1 - \frac{2\zeta(1+m_0)}{m_0(2+m_0)} \right) - \frac{1}{24m_2} + \frac{1}{16m^3} \right], \quad (20)$$

$$d_7 = \frac{2(1+m_0)}{(m_0^2+2m_0+2)} \left[ -\frac{1}{16m_3m_{\alpha E}^2} + \frac{\zeta^2 c_E}{4m_0(2+m_0)} - \frac{\zeta c_{EE}(m_0^2+2m_0+2)}{2m_0(1+m_0)(2+m_0)} - \frac{d_E}{4} \left( d_1 - \frac{2\zeta(1+m_0)}{m_0(2+m_0)} \right) - \frac{1}{24m_B} + \frac{1}{16m^3} \right]. \quad (21)$$

The parameters  $d_1$ ,  $d_2$ ,  $d_3$ , and  $d_4$  are determined by matching the zero-gluon (current) vertex. The remaining parameters are determined by matching the one-gluon (current) vertex. The result for  $d_5$  appears very different from that obtained from our previous matching calculation [12]. In fact the results are identical after matching. The result for  $d_{r_E}$  is modified by the addition of the  $d_6$  operator to the improved quark field, which makes our previous calculation of  $d_{r_E}$  [12] obsolete. As noted in Ref. [12], the result for  $d_E$  is different from that given in Ref. [6]. We anticipate that matching the four-quark matrix elements *via* NRQCD, in analogy with the matching calculation *via* HQET reported here, will yield the same results as in Ref. [6].

Finally, we note that the matching conditions yield about 150 constraints for the 13 improvement parameters  $d_i$ . These constraints also involve the coefficients in the improvement terms of the OK action. The results of the matching calculation reported here, together with the OK-action coefficients, are consistent with all the constraints. The results of this paper are being used to calculate semileptonic form factors for  $\bar{B} \rightarrow D^* \ell \bar{\nu}$  decay [15]. Meanwhile, additional cross checks are underway to confirm the results.

## Acknowledgements

The research of W. Lee is supported by the Creative Research Initiatives Program (No. 2017013332) of the NRF grant funded by the Korean government (MEST). W. Lee would like to acknowledge the support from the KISTI supercomputing center through the strategic support program for the supercomputing application research (No. KSC-2015-G2-002). Computations were carried out on the DAVID clusters at Seoul National University. J.A.B. is supported by the Basic Science Research Program of the National Research Foundation of Korea (NRF) funded by the Ministry of Education (No. 2015024974).

## A Lattice HQET vertices

In this and the following section, we omit the flavor index ( $b$  or  $c$ ) for convenience. The zero-gluon vertex of the lattice HQET Lagrangian is given by

$$\Lambda_{\text{HQ}}^{\text{lat},(0)}(p) = -\frac{1}{2m_2} p^2 + \frac{1}{8m_4^3} (p^2)^2 + \frac{1}{6} w_4 \sum_i p_i^4, \quad (22)$$

and the one-gluon vertex is  $(-gt^a)\Lambda_{\text{HQ},\mu}^{\text{lat},(1)}(p+q, p)$ , where

$$\Lambda_{\text{HQ},4}^{\text{lat},(1)}(p+q, p) = \left[ 1 - \frac{\mathbf{q}^2 - 2i\epsilon_{ijk}q_i p_j \Sigma_k}{8m_E^2} \right], \quad (23)$$

$$\begin{aligned}
\Lambda_{\text{HQ},i}^{\text{lat},(1)}(p+q,p) = & \left[ -\frac{i}{2m_2}(2p_i+q_i) + \frac{1}{2m_B}\epsilon_{ijk}\Sigma_j q_k + \frac{q_4}{8m_E^2}(q_i + i\epsilon_{ijk}\Sigma_j(2p_k+q_k)) \right. \\
& + \frac{i(2p_i+q_i)}{8m_4^3}((\mathbf{p}+\mathbf{q})^2 + \mathbf{p}^2) - \frac{1}{8m_{B'}^3}\epsilon_{ijk}\Sigma_j q_k((\mathbf{p}+\mathbf{q})^2 + \mathbf{p}^2) + \frac{i}{6}w_4(2p_i+q_i)((p_i+q_i)^2 + p_i^2) \\
& - \frac{i}{8}w_B(p_i\mathbf{q}^2 - q_i\mathbf{p}\cdot\mathbf{q}) - \frac{1}{16}w_B\epsilon_{ijk}\Sigma_j q_k\mathbf{q}^2 - \frac{1}{8}w_B\epsilon_{ijk}q_j p_k \boldsymbol{\Sigma} \cdot (2\mathbf{p}+\mathbf{q}) - \frac{1}{12}w'_B\epsilon_{ijk}\Sigma_j q_k(q_i^2 + q_k^2) \\
& \left. - \frac{1}{12}(w_4 + w'_4)\epsilon_{ijk}\Sigma_j q_k((3p_i^2 + 3p_i q_i + q_i^2) + (3p_k^2 + 3p_k q_k + q_k^2)) \right]. \quad (24)
\end{aligned}$$

The zero-gluon vertex of the lattice HQET flavor-changing current is

$$R_{\text{HQ}}^{\text{lat},(0)}(p) = 1 - \frac{i}{2m_3}\boldsymbol{\gamma} \cdot \mathbf{p} - \frac{1}{8m_{D_\perp}^2}\mathbf{p}^2 + \frac{3i\boldsymbol{\gamma} \cdot \mathbf{p}}{16m_{D_\perp}^3}\mathbf{p}^2 - dw_1 \sum_j i\gamma_j p_j^3, \quad (25)$$

and the one-gluon vertex is  $(-gt^a)R_{\text{HQ},\mu}^{\text{lat},(1)}(p+q,p)$ , with

$$R_{\text{HQ},4}^{\text{lat},(1)}(p+q,p) = -\frac{i\boldsymbol{\gamma} \cdot \mathbf{q}}{4m_{\alpha E}^2} + \frac{q_4\boldsymbol{\gamma} \cdot \mathbf{q}}{8m_{\alpha EE}^3} - \frac{(q^2 - 2i\epsilon_{ijk}\Sigma_i q_j p_k)}{16m_{\alpha rE}^3} - \frac{(q^2 + 2\mathbf{p} \cdot \mathbf{q})}{16m_6^3}, \quad (26)$$

$$\begin{aligned}
R_{\text{HQ},i}^{(1)}(p+q,p) = & \frac{1}{2m_3}\gamma_i + \frac{iq_4}{4m_{\alpha E}^2}\gamma_i - \frac{i}{8m_{D_\perp}^2}(2p_i+q_i) + \frac{\epsilon_{ijk}\Sigma_j q_k}{8m_{SB}^2} - \frac{q_4^2}{8m_{\alpha EE}^3}\gamma_i \\
& - \frac{3}{32m_{D_\perp}^3}(\boldsymbol{\gamma} \cdot (2\mathbf{p}+\mathbf{q})(2p_i+q_i) + (\mathbf{p}^2 + (\mathbf{p}+\mathbf{q})^2)\gamma_i) - \frac{3i\epsilon_{ijk}q_k}{32m_5^3}(\Sigma_j \boldsymbol{\gamma} \cdot \mathbf{p} + \boldsymbol{\gamma} \cdot (\mathbf{p}+\mathbf{q})\Sigma_j) \\
& + \frac{q_4}{16m_{\alpha rE}^3}(i\epsilon_{ijk}\Sigma_j(2p_k+q_k) + q_i) + \frac{q_4}{16m_6^3}(2p_i+q_i) + \frac{q_4}{16m_7^3}i\epsilon_{ijk}\Sigma_j q_k \\
& + dw_1\gamma_i(3p_i^2 + 3p_i q_i + q_i^2) + \frac{dw_2}{8}(\mathbf{q} \cdot (2\mathbf{p}+\mathbf{q})\gamma_i + \boldsymbol{\gamma} \cdot \mathbf{q}(2p_i+q_i)). \quad (27)
\end{aligned}$$

## B Short-distance coefficients

The explicit formulas for the lattice mass parameters  $m_i$  and the parameters  $w_i$  which appear in (22)-(24) are given in Ref. [8]. The other mass parameters and parameters  $dw_i$  which appear in (25)-(27) are as follows.

$$\frac{1}{2m_3} = \frac{\zeta(1+m_0)}{m_0(2+m_0)} - d_1, \quad \frac{1}{4m_{\alpha E}^2} = \frac{(1+m_0)\zeta}{m_0^2(2+m_0)^2} + \frac{(1+m_0)\zeta c_E}{2m_0(2+m_0)} + \frac{d_E}{2}, \quad (28)$$

$$\frac{1}{8m_{D_\perp}^2} = -\frac{\zeta(1+m_0)}{m_0(2+m_0)}d_1 + \frac{r_s\zeta}{4(1+m_0)} + \frac{\zeta^2(1+m_0)^2}{2m_0^2(2+m_0)^2} + \frac{d_2}{2}, \quad (29)$$

$$\frac{1}{8m_{SB}^2} = -\frac{\zeta(1+m_0)}{m_0(2+m_0)}d_1 + \frac{c_B\zeta}{4(1+m_0)} + \frac{\zeta^2(1+m_0)^2}{2m_0^2(2+m_0)^2} + \frac{d_B}{2}, \quad (30)$$

$$\frac{1}{16m_{\alpha rE}^3} = \frac{1}{16m_3m_{\alpha E}^2} + \frac{d_1 d_E}{4} - d_{rE}, \quad (31)$$

$$\frac{1}{16m_{\alpha EE}^3} = \frac{(1+m_0)(m_0^2+2m_0+2)\zeta}{4m_0^3(2+m_0)^3} + \frac{(1+m_0)\zeta c_E}{4m_0^2(2+m_0)^2} + \frac{(m_0^2+2m_0+2)c_{EE}}{4m_0(2+m_0)} - \frac{(m_0^2+2m_0+2)d_{EE}}{4(1+m_0)}, \quad (32)$$

$$\frac{3}{16m_{\gamma DD_\perp}^3} = \frac{\zeta^3(m_0^3 + 3m_0^2 + 5m_0 + 3)}{2m_0^3(2 + m_0)^3} + \frac{r_s \zeta^2(3m_0^2 + 6m_0 + 4)}{4m_0^2(2 + m_0)^2} + \frac{2(1 + m_0)c_2}{m_0(2 + m_0)} - \frac{(1 + m_0)^2 \zeta^2}{2m_0^2(2 + m_0)^2} d_1 - \frac{r_s \zeta}{4(1 + m_0)} d_1 + \frac{(1 + m_0) \zeta d_2}{2m_0(2 + m_0)} - d_4, \quad (33)$$

$$\frac{3}{16m_5^3} = \frac{\zeta^3(m_0^3 + 3m_0^2 + 5m_0 + 3)}{2m_0^3(2 + m_0)^3} + \frac{c_B \zeta^2(3m_0^2 + 6m_0 + 4)}{4m_0^2(2 + m_0)^2} + \frac{2(1 + m_0)c_3}{m_0(2 + m_0)} - \frac{(1 + m_0)^2 \zeta^2}{2m_0^2(2 + m_0)^2} d_1 - \frac{c_B \zeta}{4(1 + m_0)} d_1 + \frac{(1 + m_0) \zeta d_B}{2m_0(2 + m_0)} - 2d_5, \quad (34)$$

$$\frac{1}{16m_6^3} = \frac{1}{16m_3 m_{\alpha E}^2} - \frac{\zeta^2 c_E}{4m_0(2 + m_0)} + \frac{\zeta c_{EE}(m_0^2 + 2m_0 + 2)}{2m_0(1 + m_0)(2 + m_0)} + \frac{d_E}{4} \left( d_1 - \frac{2\zeta(1 + m_0)}{m_0(2 + m_0)} \right) + \frac{1}{24m_2} + \frac{(m_0^2 + 2m_0 + 2)}{2(1 + m_0)} d_6, \quad (35)$$

$$\frac{1}{16m_7^3} = \frac{1}{16m_3 m_{\alpha E}^2} - \frac{\zeta^2 c_E}{4m_0(2 + m_0)} + \frac{\zeta c_{EE}(m_0^2 + 2m_0 + 2)}{2m_0(1 + m_0)(2 + m_0)} + \frac{d_E}{4} \left( d_1 - \frac{2\zeta(1 + m_0)}{m_0(2 + m_0)} \right) + \frac{1}{24m_B} + \frac{(m_0^2 + 2m_0 + 2)}{2(1 + m_0)} d_7, \quad (36)$$

$$dw_1 = d_3 + d_1 - w_3, \quad dw_2 = \frac{\zeta^2(r_s - c_B) + 2\zeta(d_2 - d_B)(1 + m_0)}{m_0(2 + m_0)}. \quad (37)$$

## References

- [1] Y.C. Jang, W. Lee, S. Lee, J. Leem, *Update on  $\varepsilon_K$  with lattice QCD inputs*, in *Proceedings, 35th International Symposium on Lattice Field Theory (Lattice2017): Granada, Spain*, to appear in EPJ Web Conf., 1710.06614
- [2] J.A. Bailey et al. (Fermilab Lattice, MILC), Phys. Rev. **D89**, 114504 (2014), 1403.0635
- [3] J.A. Bailey et al. (MILC), Phys. Rev. **D92**, 034506 (2015), 1503.07237
- [4] H. Na, C.M. Bouchard, G.P. Lepage, C. Monahan, J. Shigemitsu (HPQCD), Phys. Rev. **D92**, 054510 (2015), [Erratum: Phys. Rev.D93,no.11,119906(2016)], 1505.03925
- [5] B. Sheikholeslami, R. Wohlert, Nucl. Phys. **B259**, 572 (1985)
- [6] A.X. El-Khadra et al., Phys. Rev. **D55**, 3933 (1997), hep-lat/9604004
- [7] A.S. Kronfeld, Phys. Rev. **D62**, 014505 (2000), hep-lat/0002008
- [8] M.B. Oktay, A.S. Kronfeld, Phys. Rev. D **78** (2008)
- [9] E. Eichten, B.R. Hill, Phys. Lett. **B234**, 511 (1990)
- [10] G.P. Lepage et al., Phys. Rev. **D46**, 4052 (1992), hep-lat/9205007
- [11] J.A. Bailey et al. (2017), [accepted to Eur. Phys. J. C], 1701.00345
- [12] J.A. Bailey, J. Leem, W. Lee, Y.C. Jang, PoS **LATTICE2016**, 285 (2016), 1612.09081
- [13] S. Balk, J.G. Korner, D. Pirjol, Nucl. Phys. **B428**, 499 (1994), hep-ph/9307230
- [14] A.V. Manohar, Phys. Rev. **D56**, 230 (1997), hep-ph/9701294
- [15] J.A. Bailey, T. Bhattacharya, R. Gupta, Y.C. Jang, W. Lee, J. Leem, S. Park, B. Yoon, *Calculation of  $\bar{B} \rightarrow D^* \ell \bar{\nu}$  form factor at zero recoil using the Oktay-Kronfeld action*, in *Proceedings, 35th International Symposium on Lattice Field Theory (Lattice2017): Granada, Spain*, to appear in EPJ Web Conf., 1710.01786